

## WAVES RESULTING FROM PARTIAL DAM BREAK WITH THE FORMATION OF A BREACH IN THE FORM OF A CUT TO THE CHANNEL BOTTOM

A. V. Chebotnikov

UDC 627.43:53.072.12

*This paper gives experimental data on the propagation speed and height of a dam-break wave arising in the tailwater region during a partial dam break event. These data were used to confirm the Khristianovich calculation method.*

**Key words:** *partial dam break, breach, discharge coefficient, dam-break wave, propagation speed.*

As is known, during a dam break event, a smooth level depression wave propagates in the headwater region and a dam-break wave propagates in the tailwater region. The characteristics of these waves depend on the initial depths of the headwater and tailwater regions and on the shape and sizes of the hole (breach) formed. The case of a total dam break, which is characteristic of high-pressure arch dams, has been well studied both theoretically [1, 2], and experimentally [3, 4]. An example of such break events is the break of the arch dam 65 m high in Malpasset (France) on December 2, 1959 [5]. However, more often, dams break only partially. A method for calculating partial dam break waves is proposed in [1].

The present paper reports the results of an experimental study of the waves resulting from a partial break of a model dam. The flow pattern near the breach was considered in [6, 7]. The parameters of dam-break waves were studied in [8]. In those papers, the breach width was significantly smaller than the channel width and the breach crest elevated above channel bottom. In practice, earth dams break more often. In this case, as a rule, the breach has the shape of a narrow cut to the channel bottom. Exactly this breach shape is considered in the present paper.

A diagram of the experiment is given in Fig. 1. The experiments were performed in a rectangular channel 16 m long, 0.38 m wide, and 0.5 m high with an even horizontal bottom. At a distance of 6.9 m upstream from the channel exit, there was a dam with a rectangular cut of width  $b = 0.06$  m symmetric about the channel walls. The thickness of the dam along the channel was  $l = 0.8$  m. The initial difference between the headwater depth  $h_-$  and the tailwater depth  $h_+$  was produced by a vertical board located near the back side of the dam. At the time  $t = 0$ , the board was quickly (in 0.05–0.10 sec) lifted vertically upward. The position of the rectangular coordinate system used further is shown in Fig. 1.

The experiments showed that, depending on the ratio of the given parameters in the problem considered, the dam-break wave can have the form of one hydraulic jump or two hydraulic jumps moving one after the other. The same types of dam-break wave occur in the case of a discontinuity decay above a drop of a channel bottom [9–11]. Below, a wave with one hydraulic jump will be called a wave of type A and a wave with two jumps will be called a wave of type B. In Fig. 1, the following notation is used:  $D_2 > 0$ ,  $0 \leq D_1 < D_2$ , and  $D_3 < 0$  are the speeds of propagation of the first and second jumps and the depression wave, respectively, and  $h_2$  and  $h_1$  are the depth of the first and second jumps, respectively. Transition from a wave of type B to a wave of type A is defined by the conditions  $D_1 = 0$  and  $h_1 = h_2$ . In the case of a total dam break, only one hydraulic jump propagates in the tailwater region.

---

Novosibirsk State University of Architecture and Building, Novosibirsk 630008; abdula111ster@gmail.com. Translated from *Prikladnaya Mekhanika i Tekhnicheskaya Fizika*, Vol. 50, No. 3, pp. 97–103, May–June, 2009. Original article submitted February 21, 2008.

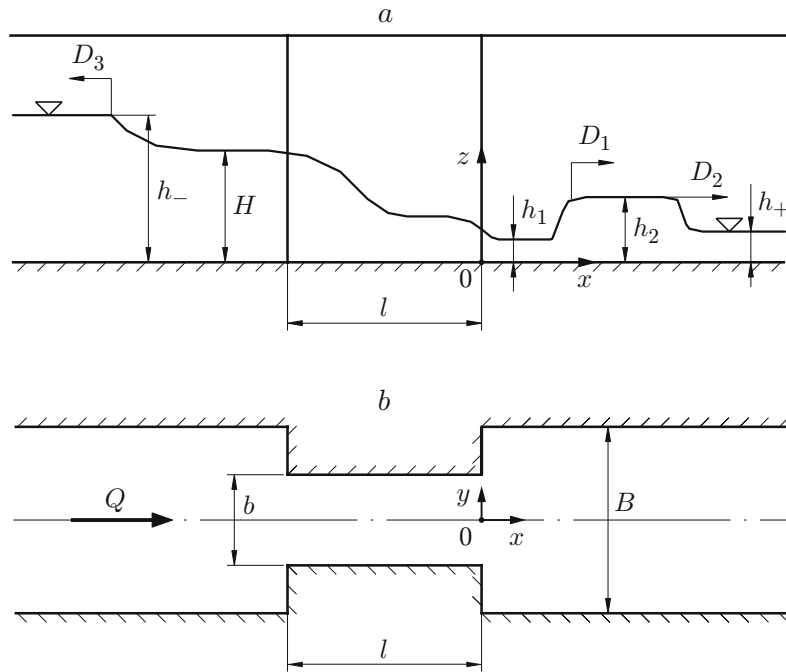


Fig. 1. Diagram of the breach and notation: (a) longitudinal section; (b) top view.

According to the first shallow water approximation [1, 2], the discontinuous waves corresponding to hydraulic jumps instantaneously become steady-state, i.e., they propagate at constant speeds without shape changes. In practice, the formation of the steady-state flow pattern is not instantaneous, and constant values of the dam-break wave parameters are reached only at a distance from the dam. In the present experiments, this distance did not exceed 2 m. The dam-break wave parameters were determined at  $x > 2$  m.

Oscillations of the free surface level on the symmetry axis of the channel for a number of fixed values of the coordinate  $x$  were measured by wavemeters operating on the principle of a significant difference in electric conductivity between air and water. Electrical conductivity was measured between two electrodes located in a plane perpendicular to the wave front. The electrodes were Nichrome wires of diameter 0.35 mm parallel to each other. The distance between the wires was 5 mm.

Static calibration of the wavemeters was carried out directly on the experimental facility by stepwise changing the depth of the quiescent liquid. The wavemeters determined a level change of 0.3 mm with an error not more than 3%. The frequency characteristics of the wavemeters were determined during sinusoidal oscillations of their electrodes at a given frequency in the quiescent liquid. It was found that the characteristic eigenfrequency of the wavemeters was  $32 \text{ sec}^{-1}$  and the attenuation decrement was  $69 \text{ sec}^{-1}$ . The corresponding amplitude–frequency characteristic  $A^0(f)$  ( $f$  is the frequency of oscillations of the electrodes) is given in Fig. 2 (curve 1). This characteristic was normalized by its value for  $f = 0$ .

During the experiments, a spectral analysis of the waves was performed. A typical curve of the modulus of the wave spectrum normalized by its value for  $f = 0$  versus frequency  $|F^0(f)|$  is given in Fig. 2 (curve 2). A comparison of the modulus of the wave spectrum and the amplitude–frequency characteristic of the wavemeters shows that the measurements error due to the frequency of oscillations of the measuring system did not exceed 1%. The electric signals of the wavemeters were entered into a computer by means of a 12-digit analog-to-digital converter.

To perform calculations using the method of [1], one should specify an experimental value of the discharge coefficient for steady-state flow through spillways in the form of a breach. Data on the discharge coefficient for typical spillways are contained in reference books on hydraulics; for the case of flow through a cut to the channel bottom, these data are limited [12, 13]. Therefore, measurements of the discharge coefficient for the breach considered were included in the program of the experiments. The steady-state discharge was measured using a standard measuring sharp-edged spillway, and the headwater and tailwater levels were determined by standard measuring needles.

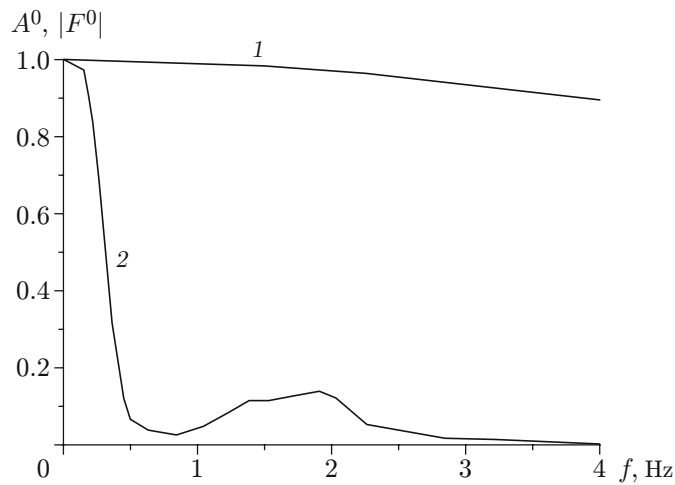


Fig. 2. Amplitude–frequency characteristic of the wavemeter (curve 1) and the modulus of the wave spectrum (curve 2) at  $h_- = 37$  cm and  $h_+ = 14.4$  cm.

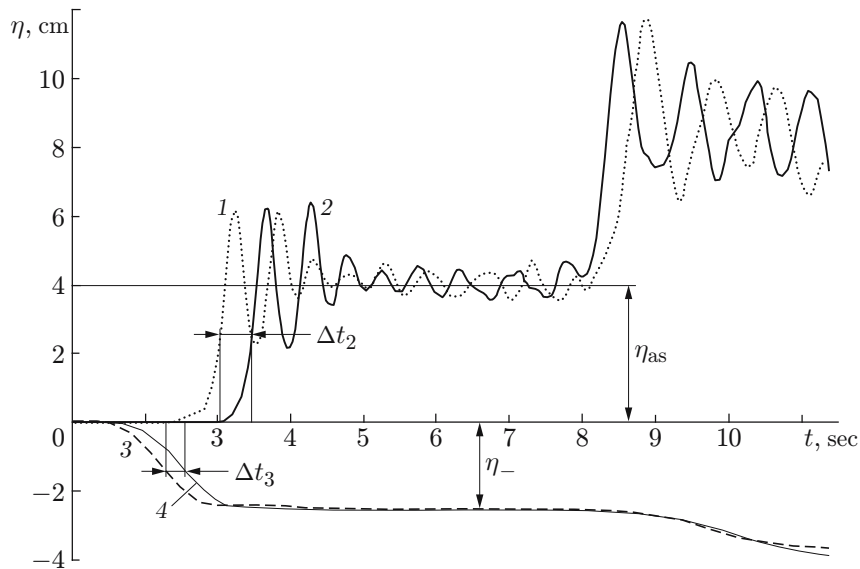


Fig. 3. Deviation of the free surface level from the initial position ( $h_- = 37$  cm and  $h_+ = 14.4$  cm):  $x = 3.21$  (1)  $3.71$  (2),  $-2.34$  (3), and  $-2.84$  m (4).

The propagation speed of the waves was determined from the signals of two motionless wavemeters shifted by a given distance  $\Delta x$ . This speed was calculated by the formula  $D_i = \Delta x_i / \Delta t_i$ , where  $\Delta t_i$  is the time required for the mid-height point of the wave front to travel a distance  $\Delta x_i$ .

An example of oscillations of the free surface level recorded synchronously by four wavemeters is given in Fig. 3. The time  $t$  reckoned from the moment of emergence of the lower edge of the board from water is plotted on the abscissa, and the deviation  $\eta$  of the free surface level from its initial position is plotted on the ordinate. The characteristic values of  $\Delta t_2$  and  $\Delta t_3$  given in Fig. 3 were used to calculate the speeds of propagation of the dam-break wave and the level depression wave.

The wavemeters were located in the tailwater region; the distance between wavemeter 1 ( $x = 3.21$  m), and wavemeter 2 was  $\Delta x = 0.5$  m. Records of signals of these wavemeters are given in Fig. 3 (curves 1 and 2, respectively). The first level rise recorded by wavemeters 1 and 2 is due to the passage of the dam-break wave, and the second level rise is due to the arrival of the reflected wave. The leading edge of the dam-break wave is followed by significant undulations. Figure 3 shows the characteristic height of the dam-break wave  $\eta_{as}$ . This quantity

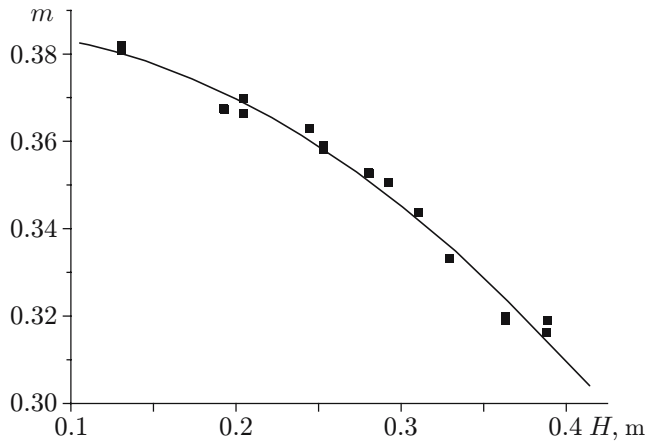


Fig. 4

Fig. 4. Discharge coefficient through the breach versus pressure: the points are experimental data; the curve is an approximation.

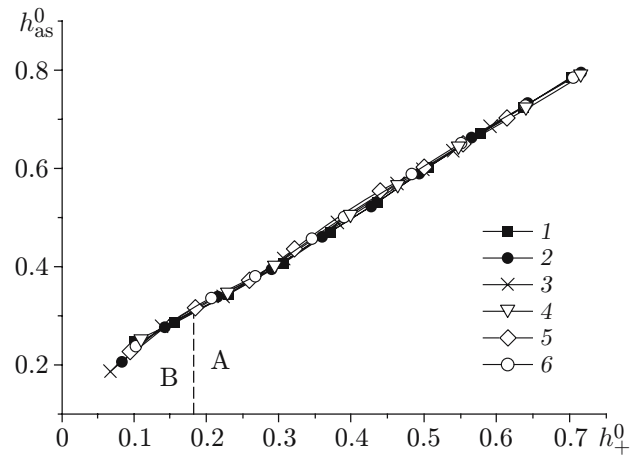


Fig. 5

Fig. 5. Depth behind the leading edge of a dam-break wave:  $h_- = 17.7$  (1),  $21.5$  (2),  $25.4$  (3),  $28.6$  (4),  $33.1$  (5), and  $37$  cm (6); a vertical dashed curve is the boundary between the regions of existence of waves of type A and B.

and the initial tailwater depth  $h_+$  were used to calculate the asymptotic depth behind the leading edge of the dam-break wave  $h_{as} = h_+ + \eta_{as}$ . Wavemeters 3 and 4 located in the headwater region at distances  $x_3 = -2.34$  m and  $x_4 = -2.84$  m (curves 3 and 4 in Fig. 3) recorded the level depression wave. The secondary level depression recorded by these wavemeters is due to the fact that the headwater length in the experiments was finite.

From Fig. 3, it follows that the flow pattern in the vicinity of the cut becomes steady-state rather rapidly although, generally, the flow remains unsteady because new portions of quiescent liquid are continuously set in motion. This confirms the assumption used in the method of [1] that the discharge of the liquid entering the tailwater region can be calculated from the discharge coefficient for a spillway in the form of a breach with steady-state flow through it.

Experimental data on the discharge coefficient for steady-state flow through the breach considered are given in Fig. 4. The abscissa shows the depth ahead of the breach  $H$  in dimensional form. This is due to the fact that, the problem of flow through spillways usually contains several geometrical parameters, and it seems impossible to combine them into a universal dimensionless complex (argument). The solid curve in Fig. 4 was obtained by least-squares approximation of experimental values by the formula

$$m = 0.385 - 0.033H - 0.557H^2.$$

In this formula, the quantity  $H$  is in meters. The data given in Fig. 4 are in good agreement with data [13]. The concrete dimensions of the cut considered in the present paper influence only the values of the coefficients in the given formula.

It should be taken into account that, in the partial dam break problem, the steady-state discharge of the liquid entering the tailwater region is determined not by the initial headwater depth  $h_-$  but by the quantity  $H = h_- - \eta_-$ , where  $\eta_-$  is the asymptotic level depression ahead of the breach (see Fig. 3). The method for calculating the quantity  $\eta_-$  proposed in [1] was confirmed in the present experiments.

Figure 5 gives experimental curves of the depth  $h_{as}^0 = h_{as}/h_-$  behind the leading edge of the dam-break wave versus initial tailwater depth  $h_+^0 = h_+/h_-$ . If we ignore the relatively small oscillations of the free surface level occurring in experiments after degeneration of undulations, the depth  $h_{as}$  will have the same value as the calculated depth  $h_2$  (see Fig. 1). The experiments were performed for six values of  $h_-$ . The dimensionless parameters  $B/h_-$ ,  $b/h_-$ , and  $l/h_-$  ( $B$  is the channel width) were varied in the following ranges:  $1.00 \leq B/h_- \leq 2.15$ ,  $0.16 \leq b/h_- \leq 0.34$ , and  $2.16 \leq l/h_- \leq 4.52$ . From Fig. 5, it follows that the quantity  $h_{as}^0$  is almost independent of  $h_-$  in the range of this parameter considered.

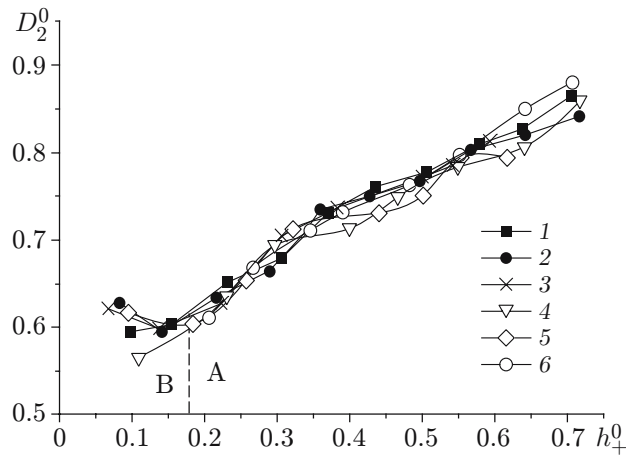


Fig. 6. Propagation speed of the leading edge of the dam-break wave (the notation the same as in Fig. 5).

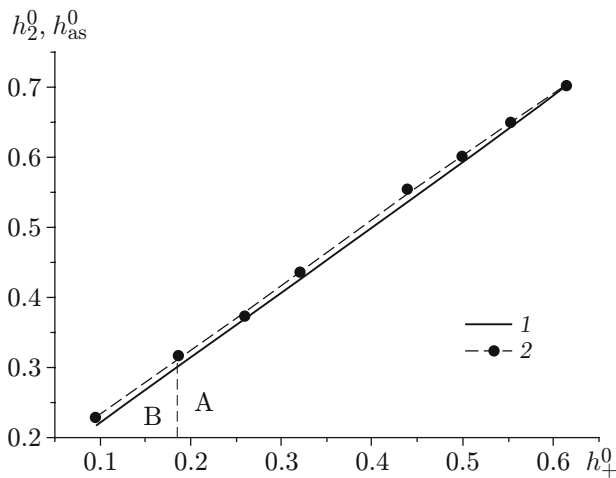


Fig. 7

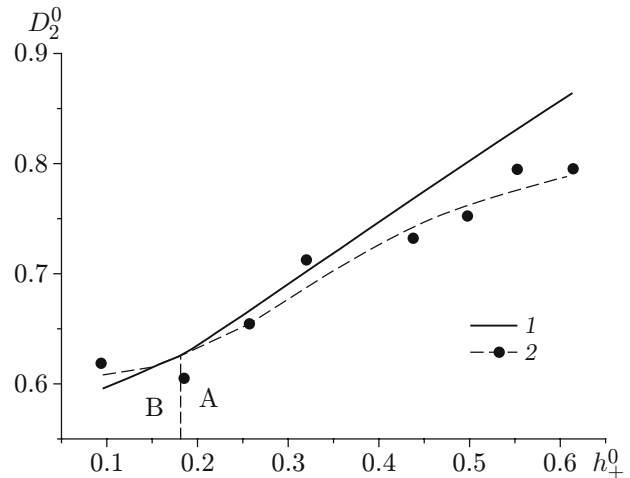


Fig. 8

Fig. 7. Depth behind the leading edge of the dam-break wave at  $h_- = 33.1$  cm: 1) results of calculations using the method of [1]; 2) experimental data; the vertical dashed line is the boundary of the regions of existence of waves of type A and B.

Fig. 8. Propagation speed of the leading edge of the dam-break wave at  $h_- = 33.1$  cm (notation the same as in Fig. 7).

The dimensionless propagation speeds of the leading edge of the dam-break wave obtained in the experiments  $D_2^0 = D_2/(gh_-)^{1/2}$  are given in Fig. 6. The spread of the experimental values of  $D_2^0$  obtained for various values of the dimensionless parameters of the cut is more significant than the spread of the values of  $h_{as}^0$ . However, if an error not exceeding 5% is admissible, this spread can be ignored.

The obtained experimental data can be used to verify various calculation methods. Figure 7 and 8 gives the results of a series of experiments and calculations using the method of [1]. In the calculations performed using this method, the propagation speed of the leading edge of the dam-break wave is slightly overestimated and the depth behind the leading edge is underestimated. However, the difference of the results is insignificant. Similar results were obtained by comparing available data with those obtained in other series of experiments.

This work was supported by the Russian Foundation for Basic Research (Grant No. 07-01-00015) and the Federal Agency on Education of the Russian Federation (direction No. 2.1.2).

## REFERENCES

1. S. A. Khristianovich, S. G. Mikhlin, and B. B. Devison, "Unsteady motion in channels and rivers," in: *Some New Problems of the Mechanics of Continuous Media* [in Russian], Izd. Akad. Nauk SSSR (1938), pp. 15–154.
2. J. J. Stoker, *Water Waves Wiley*, New York (1992).
3. R. F. Dressler, "Comparison of theories and experiments for the hydraulic dam-break wave," *Int. Assoc. Sci. Hydrology*, **3**, No. 38, 319–328 (1954).
4. V. I. Bukreev, A. V. Gusev, A. A. Malysheva, and I. A. Malysheva, "Experimental verification of the gas-hydraulic analogy using the dam break problem as an example," *Izv. Ross. Akad. Nauk, Mekh. Zhidk. Gaza*, **5**, 143–152 (2004).
5. A. Valiani, V. Caleffi, and A. Zanni, "Case study: malpasset dam-break simulation using a two-dimensional finite volume method," *J. Hydraulic Eng.*, **128**, Part 5, 460–472 (2002).
6. V. I. Bukreev, "On the water depth in the breach in a partial dam break event," *Izv. Ross. Akad. Nauk, Mekh. Zhidk. Gaza*, **5**, 115–123 (2005).
7. V. I. Bukreev, "On the discharge characteristic at the dam site after dam break," *J. Appl. Mech. Tech. Phys.*, **47**, No. 5, 679–687 (2006).
8. A. V. Chebotnikov, "Waves from partial dam breaks: Experiment," *Izv. Vyssh. Uchebn. Zaved., Stroitel'stvo*, **2**, 57–62 (2008).
9. V. V. Ostapenko, "Discontinuous solutions of the shallow water equations for flow over a bottom step," *J. Appl. Mech. Tech. Phys.*, **43**, No. 6, 836–846 (2002).
10. V. I. Bukreev and A. V. Gusev, "Gravity waves due to discontinuity decay over an open channel bottom drop," *J. Appl. Mech. Tech. Phys.*, **44**, No 4, 506–515 (2003).
11. V. I. Bukreev, A. V. Gusev, and V. V. Ostapenko, "Free surface discontinuity decay above a channel bottom drop," *Izv. Ross. Akad. Nauk, Mekh. Zhidk. Gaza*, No. 6, 72–83 (2003).
12. R. R. Chugaev, *Hydraulics* [in Russian], Énergoizdat, Leningrad (1982).
13. P. G. Kiselev, *Handbook on Hydraulic Calculations* [in Russian], Énergiya, Moscow (1972).